



# Fourier transform emission spectroscopy of the near infrared transitions of CeS



R.S. Ram<sup>a,\*</sup>, P.F. Bernath<sup>a,b</sup>

<sup>a</sup>Department of Chemistry, University of York, Heslington, York YO10 5DD, UK

<sup>b</sup>Department of Chemistry and Biochemistry, Old Dominion University, Norfolk, VA 23529, USA

## ARTICLE INFO

### Article history:

Received 17 October 2013

In revised form 10 March 2014

Available online 20 March 2014

### Keywords:

CeS

Lanthanide sulfides

Emission spectroscopy

Electronic transition

Rotational analysis

Spectroscopic constants

## ABSTRACT

The emission spectra of CeS have been investigated at high resolution with a Fourier transform spectrometer. Several bands observed in the 4000–9000 cm<sup>-1</sup> region have been classified into nine transitions having five different lower states, X<sub>1</sub>(3), X<sub>2</sub>(≥ 2), X<sub>3</sub>(≥ 2), X<sub>4</sub>(≥ 3) and X<sub>5</sub>(0) based on Ω doubling and relative branch intensities.

Out of these, the [7.54] (4) → X<sub>1</sub>(3) transition consisting of 0–1, 1–2, 0–0, 1–1, 1–0 and 2–1 bands is strongest in intensity. A rotational analysis of these bands provides equilibrium spectroscopic constants: ω<sub>e</sub> = 461.3947(14) cm<sup>-1</sup>, ω<sub>e</sub>x<sub>e</sub> = 1.00095(65) cm<sup>-1</sup>, B<sub>e</sub> = 0.118782207(15) cm<sup>-1</sup>, α<sub>e</sub> = 0.000341453(14) cm<sup>-1</sup> and r<sub>e</sub> = 2.33522875(15) Å for the lower X<sub>1</sub>(Ω = 3) state. The [8.78] (≥ 3) → X<sub>2</sub>(≥ 2) transition, for which 0–0 and 0–1 bands were rotationally analyzed, provides ΔG<sub>1/2</sub> = 458.87411(88) cm<sup>-1</sup>, B<sub>e</sub> = 0.1187649(31) cm<sup>-1</sup>, α<sub>e</sub> = 0.0003401(37) cm<sup>-1</sup> and r<sub>e</sub> = 2.335399(31) Å for the X<sub>2</sub>(Ω ≥ 2) lower state.

© 2014 Elsevier Inc. All rights reserved.

## 1. Introduction

While electronic spectra of many lanthanide-containing diatomic oxides are known, only a few diatomic sulfides such as LaS [1–4], YbS [5,6] and HoS [7] have been investigated in the gas phase. The spectra of lanthanide-containing molecules are very complex with a high density of states resulting from partially filled *f*-orbitals. The electronic states of these molecules are Hund's case (c) states in which the spin components are widely separated and only their Ω values remain as good quantum numbers. For most lanthanide sulfides no spectroscopic data are available and in some cases where data are available, knowledge of the low-lying electronic states remains fragmentary.

Among the cerium-containing molecules the electronic spectra of only CeO and CeF have been investigated to date. CeO has been investigated in detail, first by conventional spectroscopy [8], and later by laser excitation spectroscopy [9–13] and many low-lying electronic states have been identified. The experimental observations have been supported by several theoretical studies [14–16]. The electronic spectra of CeF have also been investigated in previous experimental studies [17,18].

CeO has been of considerable interest because of its astrophysical importance. This molecule has been identified in the spectra of S-type stars by several workers [19–22] and there is a strong

possibility that CeS might also be found. So far no experimental observations have been reported, and no experimental spectroscopic constants are available for CeS. Coppens et al. [23] have provided estimated values of the vibrational constant ω<sub>e</sub> = 510 cm<sup>-1</sup> and bond length r<sub>e</sub> = 2.15 Å based on CeO. They have also reported the dissociation energy D<sub>0</sub> = 126 kcal/mol for CeS. In recent density function calculations on lanthanide monosulfides, Luo et al. [24] have predicted ω<sub>e</sub> = 426 cm<sup>-1</sup> and r<sub>e</sub> = 2.36 Å for CeS while a vibrational frequency of ω<sub>e</sub> = 457 cm<sup>-1</sup> has been provided [25] by some primitive calculations.

The present work has been motivated by the need to obtain spectroscopic parameters of CeS in the gas phase because of its potential astrophysical importance. In the present paper we report on the identification of a number of transitions of CeS in the near infrared, with their 0–0 bands located near 4374, 4741, 6491, 7541, 7678, 6026, 8428, 8676 and 8781 cm<sup>-1</sup>. A tentative Ω-assignment of the observed states has been proposed based on the magnitude of the Ω-doubling and the relative intensity of the Q, R and P branches in different bands.

## 2. Experimental

The spectra of CeS used in the present analysis were recorded by S.P. Davis in thermal emission on 01/17/1989 [spectrum #890117R0.002] at Kitt Peak. CeS was produced in a high temperature carbon tube furnace (King furnace) by vaporizing

\* Corresponding author. Fax: +44 0 1904 432516.

E-mail address: rr662@york.ac.uk (R.S. Ram).

Ce<sub>2</sub>S<sub>3</sub> at a temperature of ~2200 °C in an atmosphere of about 274 Torr of helium. The spectrometer was equipped with a CaF<sub>2</sub> beam splitter, Si filter and InSb detectors. The spectra in the 1850–9150 cm<sup>-1</sup> region were recorded using the 1-m Fourier transform spectrometer of the National Solar Observatory at Kitt Peak by co-adding 8 scans in about 2 h of integration at a resolution of 0.01 cm<sup>-1</sup>. The line positions were extracted using the WSPECTRA program (M. Carleer, Free University of Brussels) by fitting a Voigt line shape function to the individual spectral features. The precision of measurement is expected to be of the order of ±0.003 cm<sup>-1</sup> or better for the stronger and unblended lines. However, for rotational lines of weaker bands which are frequently overlapped by lines of stronger bands, the measurement uncertainty is expected to be of the order of ±0.005 cm<sup>-1</sup> or higher. Several new bands observed in the near infrared have been attributed to CeS based on a rotational analysis. Prior to this experiment, the furnace was used for the observation of near infrared bands of LaS; therefore, some LaS bands of the A<sup>2</sup>Π–A<sup>2</sup>Δ<sub>v</sub> transition were also present as an impurity. In addition, molecular lines belonging to the Δ<sub>v</sub> = 2 overtone bands of CO, Ballik–Ramsay system of C<sub>2</sub> and Δ<sub>v</sub> = –1 and –2 sequence bands of the A<sup>2</sup>Π<sub>i</sub>–X<sup>2</sup>Σ<sup>+</sup> transition of CN, were also present as impurities. We have used the CN lines [26] to calibrate the wavenumbers of CeS lines. The molecular lines were sorted into branches of different bands using a color Loomis program running on a PC computer and rotational assignment was made by comparing combination differences for common vibrational levels.

### 3. Description of observed spectra

The spectrum of CeS in general is weak in intensity. In spite of weak intensity, several new bands located near 4374, 4741, 6026, 6491, 7541, 7678, 8428, 8674 and 8781 cm<sup>-1</sup> have been rotationally analyzed and assigned as 0–0 bands of different transitions. A rotational analysis of some associated higher vibrational bands has also been obtained. The main features of these transitions are summarized in Table 1. Several much weaker bands still remain unanalyzed. Since the spectra were recorded using a furnace, no first lines were identified in any of the observed bands.

Spectroscopic constants for the observed states of different transitions were determined by fitting the observed rotational lines using the following simple term energy expressions:

For the Ω = 0 and Ω ≥ 2 states without observed Ω-splitting:

$$F_v(J) = T_v + B_v J(J+1) - D_v [J(J+1)]^2 + H_v [J(J+1)]^3 + L_v [J(J+1)]^4 \quad (1)$$

For Ω = 1 and higher Ω states with observed Ω-splitting:

$$F_v(J) = T_v + B_v J(J+1) - D_v [J(J+1)]^2 + H_v [J(J+1)]^3 + L_v [J(J+1)]^4 \pm 1/2 \{ q_w J(J+1) + q_{Dv} [J(J+1)]^2 + q_{Hv} [J(J+1)]^3 + q_{Lv} [J(J+1)]^4 \} \quad (2)$$

**Table 1**

Main features of CeS bands in the near infrared.

Transitions <sup>a</sup>	Main features
[4.37] (Ω = 3) → X <sub>1</sub> (Ω = 2)	1P, 1Q, 1R branches with intensity of Q > R > P, no doubling, no combination defects
[4.74] (Ω ≥ 2) → X <sub>4</sub> (Ω ≥ 3)	1P, 1Q, 1R branches with intensity of Q > P > R, no doubling, no combination defects
[6.03] (Ω = 1) → X <sub>5</sub> (Ω = 0)	1P, 1Q, 1R branches with intensity of Q > R > P, no doubling, combination defects
[6.49] (Ω = 2) → X <sub>1</sub> (Ω = 3)	2P, 2Q, 2R branches with intensity of Q > R ≈ P, no perturbations
[7.54] (Ω = 4) → X <sub>1</sub> (Ω = 3)	1P, 1Q, 1R branches with intensity of Q > R > P, no doubling no combination defects
[7.68] (Ω = 2) → X <sub>1</sub> (Ω = 3)	2P, 2Q, 2R branches with intensity of Q > R ≈ P, perturbations
[8.43] (Ω = 2) → X <sub>1</sub> (Ω = 3)	2P, 2Q, 2R branches with intensity of Q > R ≈ P, perturbations
[8.67] (Ω ≥ 3) → X <sub>3</sub> (Ω ≥ 2)	1P, 1Q, 1R branches with intensity of Q > R > P, no doubling no combination defects
[8.78] (Ω ≥ 3) → X <sub>2</sub> (Ω ≥ 2)	1P, 1Q, 1R branches with intensity of Q > R > P, no doubling no combination defects

<sup>a</sup> See the energy level diagram in Fig. 1, for lower state notations.

The rotational lines of all transitions connecting to the X<sub>1</sub>(Ω = 3) state were fitted simultaneously. Rotational lines were weighted based on their signal-to-noise ratio, extent of blending and the effects of perturbations. The spectroscopic T<sub>v</sub>, B<sub>v</sub> and D<sub>v</sub> were determined for all the lower states except for T<sub>0</sub> values which were held fixed at 0.0 cm<sup>-1</sup>. The higher order constants such as H<sub>v</sub>, L<sub>v</sub>, q<sub>v</sub>, q<sub>Dv</sub>, q<sub>Hv</sub>, q<sub>Lv</sub> were also determined for some excited states. A list of observed rotational lines of CeS bands used in the final least-squares fit along with their obs.–calc. residuals is provided on ScienceDirect ([www.sciencedirect.com](http://www.sciencedirect.com)) and as supplement-1 as part of the Ohio State University Molecular Spectroscopy Archives ([http://msa.lib.ohio-state.edu/jmsa\\_hp.htm](http://msa.lib.ohio-state.edu/jmsa_hp.htm)). The spectroscopic constants of the observed electronic states are provided in Tables 2 and 3. The molecular constants of the ν = 0, 1 and 2 vibrational levels of the X<sub>1</sub>(Ω = 3) and [7.54] (Ω = 4) states, and ν = 0 and 1 vibrational levels of the X<sub>2</sub>(Ω ≥ 2) have been used to determine the equilibrium constants for these three states, which are provided in Table 4.

A schematic energy level diagram of the assigned transitions is provided in Fig. 1. As shown in this figure, five lower states, labeled here as X<sub>1</sub>(Ω = 3), X<sub>2</sub>(Ω ≥ 2), X<sub>3</sub>(Ω ≥ 2), X<sub>4</sub>(Ω ≥ 3), and X<sub>5</sub>(Ω = 0) with similar rotational constants have been identified. Of these, the X<sub>1</sub> and X<sub>2</sub> lower states have similar ΔG<sub>v/2</sub> vibrational intervals of 459.39 and 458.87 cm<sup>-1</sup>, respectively. A description of different transitions is provided in the following sections.

#### 3.1. Transitions with X<sub>1</sub>(Ω = 3) as a lower state

Rotational analysis indicates that five transitions with 0–0 bands located near 4374, 6491, 7541, 7678 and 8428 cm<sup>-1</sup> have a common lower state. The Ω-assignment of the upper and lower states of these transitions is based on the presence or absence of Ω doubling and the relative intensity of the P, Q and R branches. These transitions have been labeled as [4.37] (4) → X<sub>1</sub>(3), [6.49] (2) → X<sub>1</sub>(3), [7.54] (4) → X<sub>1</sub>(3), [7.68] (2) → X<sub>1</sub>(3) and [8.43] (2) → X<sub>1</sub>(3), where the values in square brackets are wavenumbers of the 0–0 bands in units of 10<sup>3</sup> cm<sup>-1</sup>. Of these transitions, the 7541 cm<sup>-1</sup> transition is the strongest in intensity and was analyzed in the beginning. The analysis of this transition was helpful in assigning the other transitions with the same lower state.

##### 3.1.1. The [4.37] (4) → X<sub>1</sub>(3) and [7.54] (4) → X<sub>1</sub>(3) transitions

The 4374 and 7541 cm<sup>-1</sup> bands consist of a single P, Q and R branches (with intensity as Q > R > P) without any doubling in the lines or any combination defects. This suggests that ΔΩ = +1 transitions are involved. No Δν = ±1 or higher vibrational bands of this transition were identified in our spectra.

The 7541 cm<sup>-1</sup> transition consists of Δν = –1, 0 and 1 sequence bands and we have obtained a rotational analysis of the 0–1, 1–2, 0–0, 1–1, 1–0 and 2–1 bands. As will be described later, three other transitions having the same lower state have resolved Ω-doubling in the P, Q, R branches consistent with Ω = 2 assignment for their upper states. This observation has suggested that the X<sub>1</sub> lower state

**Table 2**  
Spectroscopic constants (in  $\text{cm}^{-1}$ ) of the  $X_1(\Omega = 3)$  and other excited states having transitions to this state.

Constants <sup>a</sup>	$X_1(\Omega = 3)$			[7.54] ( $\Omega = 4$ )		
	$\nu = 0$	$\nu = 1$	$\nu = 2$	$\nu = 0$	$\nu = 1$	$\nu = 2$
$T_v$	0.0	459.39283(43)	916.7837(12)	7540.67404(20)	7965.73117(96)	8388.5857(13)
$B_v$	0.11861148(85)	0.11827003(85)	0.11792846(98)	0.11397263(84)	0.1137035(11)	0.1134555(12)
$D_v \times 10^8$	3.1540(22)	3.1584(22)	3.1643(48)	3.2109(22)	3.060(12)	3.079(13)
$H_v \times 10^{13}$	–	–	–	–	0.760(61)	2.118(62)
Constants <sup>a,b</sup>	[4.37] ( $\Omega = 4$ ) $\nu = 0$	[6.49] ( $\Omega = 2$ ) $\nu = 0$	[7.68] ( $\Omega = 2$ ) $\nu = 0$	[8.43] ( $\Omega = 2$ ) $\nu = 0$		
$T_v$	4373.87524(53)	6490.59501(45)	7678.28874(57)	8427.74836(75)		
$B_v$	0.11403560(85)	0.11391261(86)	0.11223623(98)	0.11359469(89)		
$D_v \times 10^8$	3.2232(23)	2.9671(29)	–1.675(11)	2.9178(36)		
$H_v \times 10^{12}$	–	–0.00550(51)	–1.2931(85)	0.03501(80)		
$q_{Dv} \times 10^8$	–	0.08565(91)	–2.3333(51)	–1.4681(21)		
$q_{Hv} \times 10^{12}$	–	–0.00175(47)	1.0859(71)	0.3767(22)		

<sup>a</sup> Values in parentheses are one standard deviation error in the last digits quoted.

<sup>b</sup> Constants  $L_0 = 1.811(22) \times 10^{-17}$  and  $q_{L0} = -2.032(24) \times 10^{-17}$  for the [7.68] ( $\Omega = 2$ ) and  $q_{L0} = -2.320(58) \times 10^{-18}$  for the [8.43] ( $\Omega = 2$ ) were also determined.

**Table 3A**  
Spectroscopic constants (in  $\text{cm}^{-1}$ ) of the  $X_2(\Omega \geq 2)$ ,  $X_3(\Omega \geq 2)$ ,  $X_4(\Omega \geq 3)$  and  $X_5(0)$  lower states of CeS.

Constants <sup>a</sup>	$X_2(\Omega \geq 2) \nu = 0$		$X_3(\Omega \geq 2) \nu = 0$	$X_4(\Omega \geq 3) \nu = 0$	$X_5(0) \nu = 0$
	$\nu = 0$	$\nu = 1$	$\nu = 0$	$\nu = 0$	$\nu = 0$
$T_v$	0.0	458.87411(88)	0.0	0.0	0.0
$B_v$	0.1185948(26)	0.1182547(26)	0.1176391(83)	0.1168349(72)	0.1187740(36)
$D_v \times 10^8$	3.2080(72)	3.2160(72)	3.131(62)	6.030(43)	3.079(12)

<sup>a</sup> Values in parentheses are one standard deviation error in the last digits quoted.

**Table 3B**  
Spectroscopic constants (in  $\text{cm}^{-1}$ ) of the  $\nu = 0$  vibrational levels of the [8.78] ( $\Omega \geq 3$ ), [8.67] ( $\Omega \geq 3$ ), [4.74] ( $\Omega \geq 2$ ), [6.03] ( $\Omega = 1$ ) states of CeS.

Constants <sup>a</sup>	[8.78] ( $\Omega \geq 3$ ) $\nu = 0$	[8.67] ( $\Omega \geq 3$ ) $\nu = 0$	[4.74] ( $\Omega \geq 2$ ) $\nu = 0$	[6.03] ( $\Omega = 1$ ) $\nu = 0$
$T_v$	8780.62864(65)	8673.8453(13)	4741.1757(11)	6026.29833(82)
$B_v$	0.1119293(26)	0.1123219(84)	0.1129089(71)	0.1146220(37)
$D_v \times 10^8$	3.2915(74)	2.207(68)	–1.051(52)	2.330(13)
$H_v \times 10^{12}$	–0.00426(30)	0.173(26)	–3.038(40)	–0.1672(32)
$L_v \times 10^{17}$	–	2.038(77)	6.57(14)	0.1512(55)
$q_v \times 10^4$	–	–	–	3.3084(13)
$q_{Dv} \times 10^9$	–	–	–	–1.3710(70)

<sup>a</sup> Values in parentheses are one standard deviation error in the last digits quoted.

**Table 4**  
Equilibrium constants (in  $\text{cm}^{-1}$ ) for the observed electronic states of CeS.

Constants <sup>a</sup>	$X_1(\Omega = 3)$	$X_2(\Omega \geq 2)$	[7.54] ( $\Omega = 4$ )
$T_e$	0.0	0.0	7557.7666(13)
$\omega_e$	461.3947(14)	[458.87411(88)] <sup>b</sup>	427.2597(20)
$\omega_e x_e$	1.00095(65)	–	1.10130(87)
$B_e$	0.118782207(15)	0.1187649(31)	0.1141001(89)
$\alpha_e \times 10^3$	3.41453(14)	3.401(37)	2.596(58)
$r_e$ (Å)	2.33522875(15)	2.335399(31)	2.382660(93)

<sup>a</sup> Values in parentheses are one standard deviation error in the last digits quoted.

<sup>b</sup>  $\Delta G^\ddagger/2$  value.

must be an  $\Omega = 3$  state. A portion of the 0–0 band of this transition is presented in Fig. 2, in which some rotational lines of the R and Q branches have been marked. The P branch lines in this portion of spectrum were not resolved and have not been marked in this figure.

### 3.1.2. The [6.49] (2) $\rightarrow$ $X_1(3)$ , [7.68] (2) $\rightarrow$ $X_1(3)$ and [8.43] (2) $\rightarrow$ $X_1(3)$ transitions

The three bands located near 6491, 7678 and 8428  $\text{cm}^{-1}$  consisting of 2P, 2Q and 2R branches with  $Q > R \approx P$  in intensity. This indicates that  $\Delta\Omega = +1$  or  $-1$  transitions may be involved in

these transitions. These transitions have the same lower state as the 4374 and 7541  $\text{cm}^{-1}$  transition described earlier. A rotational analysis of the three transitions results in  $q_D$  lambda doubling constants for the upper states instead of significant values of  $q$ . The fact that the quadratic  $q_D$   $\Omega$ -doubling term in Eq. (2) is dominant indicates that upper states of these transitions have  $\Omega = 2$ .

The 0–1 and 1–0 bands of the 6490  $\text{cm}^{-1}$  transition were very weak in intensity. In spite of very weak intensity a search for the 0–1 band of this transition was made using the spectroscopic constants for the  $X_1(3) \nu = 1$  level. Based on the prediction, the  $Q_1$  and  $Q_2$  branches of the 0–1 band were easily identified in our spectra using the Loomis–Wood program and included in the final fit. The R head of this transition was also predicted and found near 6034.3  $\text{cm}^{-1}$ . The 1–0 band of this transition could not be identified. Our rotational analysis indicates that the doubling of the branches was caused entirely by  $\Omega$ -doubling in the excited state. No rotational perturbations were observed and lines as high as  $P_1(110)$ ,  $P_2(123)$ ,  $Q_1(176)$ ,  $Q_2(160)$ ,  $R_1(149)$  and  $R_2(150)$  were identified in the 0–0 band.

All of the six branches of the 7678  $\text{cm}^{-1}$  transition are affected by local perturbations. Our rotational analysis indicates that rotational perturbations occur in the excited state at different  $J$  values in the  $e$ - and  $f$ -parity levels [ $J = 58$  ( $e$ ) and 78 ( $f$ ), respectively]. Several rotational lines near the perturbation were given lower

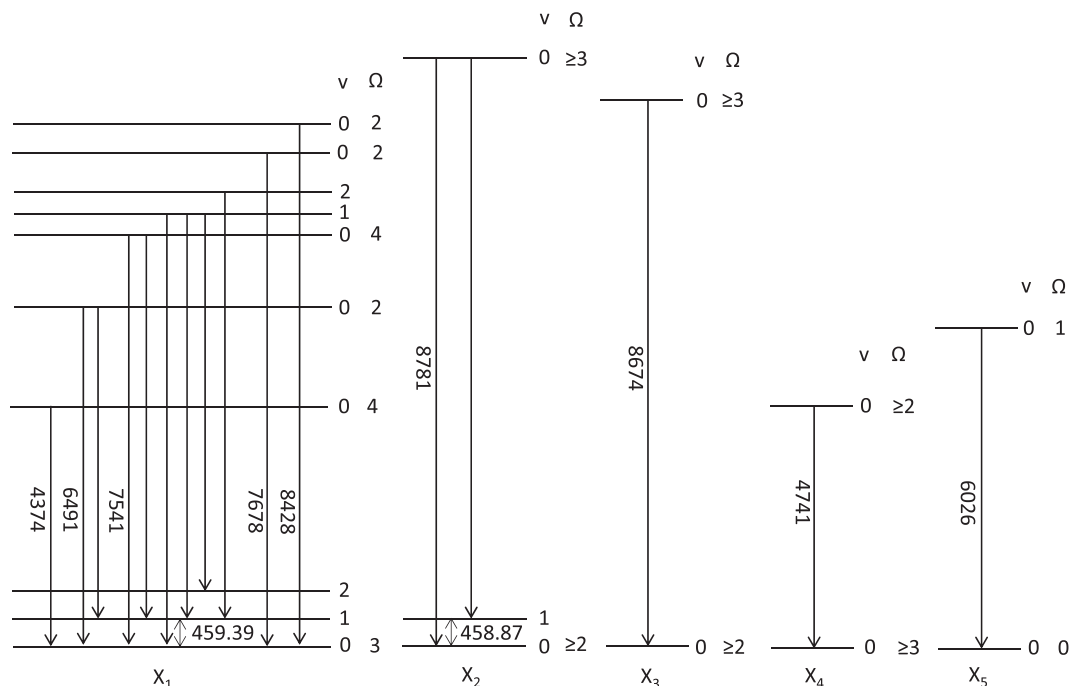


Fig. 1. Schematic energy level diagram of the near infrared transitions of CeS.

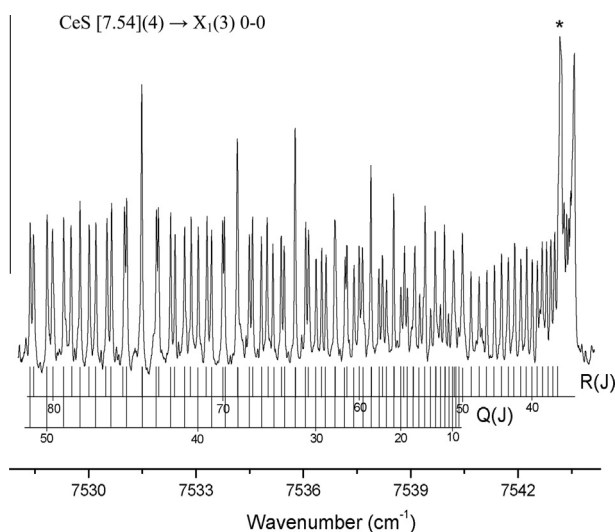


Fig. 2. A portion of the 0–0 band of the [7.54] (4)  $\rightarrow$   $X_1(3)$  transition of CeS with some R(J) and Q(J) lines marked. An asterisk marks an atomic line present near the R head.

weights or were de-weighted in the final fits. Rotational lines up to  $P_1(120)$ ,  $P_2(124)$ ,  $Q_1(154)$ ,  $Q_2(151)$ ,  $R_1(138)$  and  $R_2(118)$  were assigned. A search for the 0–1 and 1–0 bands of this transition was unsuccessful.

For the 0–0 band near  $8428\text{ cm}^{-1}$  we have assigned rotational lines up to  $P_1(148)$ ,  $P_2(142)$ ,  $Q_1(180)$ ,  $Q_2(159)$ ,  $R_1(151)$  and  $R_2(142)$ . No other band associated with this transition has been identified in our spectra.

### 3.2. Transitions with $X_2(\Omega \geq 2)$ , $X_3(\Omega \geq 2)$ , $X_4(\Omega \geq 3)$ as lower states

The  $8781$ ,  $8674$  and  $4741\text{ cm}^{-1}$  bands having the lower states  $X_2$ ,  $X_3$  and  $X_4$ , respectively, have single P, Q and R branches. The  $8781$  and  $8674\text{ cm}^{-1}$  bands (with  $Q > R > P$ ) involve  $\Delta\Omega = +1$  transitions between higher  $\Omega$  states. The  $4741\text{ cm}^{-1}$  band has intensity

$Q > P > R$  indicating that it involves a  $\Delta\Omega = -1$  transition. The three 0–0 bands have been assigned as [8.78] ( $\geq 3$ )  $\rightarrow$   $X_2(\geq 2)$ , [8.67] ( $\geq 3$ )  $\rightarrow$   $X_3(\geq 2)$  and [4.74] ( $\geq 2$ )  $\rightarrow$   $X_4(\geq 3)$  transitions. Since the case (c) states of CeS may have mixed character, relative intensity of branches especially in high  $\Omega$  transitions, may not provide correct information about their  $\Omega$  assignment.

#### 3.2.1. The [8.78] ( $\geq 3$ ) $\rightarrow$ $X_2(\geq 2)$ transition

Two bands with single P, Q, R branches, located at  $8781$  and  $8322\text{ cm}^{-1}$ , have been assigned at the 0–0 and 0–1 bands of the [8.78] ( $\geq 3$ )  $\rightarrow$   $X_2(\geq 2)$ . A rotational analysis of these two bands has provided  $\Delta G_{1/2} = 458.87\text{ cm}^{-1}$  for the  $X_2(\geq 2)$  lower state. This value is very similar to the vibrational interval  $\Delta G_{1/2} = 459.39\text{ cm}^{-1}$  of the  $X_1(3)$  lower state. No other bands having the same lower state have been identified in our spectra.

#### 3.2.2. The [8.67] ( $\geq 3$ ) $\rightarrow$ $X_3(\geq 2)$ transition

Another  $\Delta\Omega = +1$  band with single P, Q, R branches, located at  $8674\text{ cm}^{-1}$ , has different lower and upper states than the other transitions. The lower state rotational constants of this transition are  $B_0'' = 0.1176391(83)$ ,  $D_0'' = 3.131(62) \times 10^{-8}\text{ cm}^{-1}$ . This transition has been labeled as the [8.67] ( $\geq 3$ )  $\rightarrow$   $X_3(\Omega \geq 2)$ . A lower wavenumber band located at  $8634\text{ cm}^{-1}$  (with  $B = 0.1172976(76)$ ,  $D = 3.131(34) \times 10^{-8}\text{ cm}^{-1}$ ) is probably the 1–1 band associated with this transition. This assignment, however, could not be confirmed independently because the 0–1 band was not observed.

#### 3.2.3. The [4.74] ( $\geq 2$ ) $\rightarrow$ $X_4(\geq 3)$ transition

The  $4741\text{ cm}^{-1}$  band having single P, Q and R branches (with  $Q > P > R$ ), has a different lower state. This observation is consistent with the  $\Delta\Omega = -1$  assignment and this transition has been labeled as [4.74] ( $\geq 2$ )  $\rightarrow$   $X_4(\geq 3)$ .

### 3.3. Transition with $X_5(0)$ as the lower state

The  $6026\text{ cm}^{-1}$  transition consists of single P, Q and R branches showing combination defects because of appreciable  $\Omega$ -doubling in the upper state. This transition has the character of a  ${}^1\Pi - {}^1\Sigma^+$

transition and we have labeled it as the [6.03] ( $\Omega = 1$ )  $\rightarrow$   $X_5(\Omega = 0)$  transition. No perturbations have been observed and we have observed rotational lines up to P(151), Q(179) and R(155).

For the isovalent CeO, there are two low-lying  $\Omega = 0$  states,  $V_1 0^-$  and  $U_1 0^+$ , and the electronic states of CeS are expected to show a similar pattern. As there is no way to distinguish between  $0^+$  and  $0^-$  in the present analysis, the lower state has simply been labeled as  $X_5(0)$ .

#### 4. Results and discussion

Prior to the present work no experimental observations have been reported on CeS. In a recent theoretical study, density functional calculations have been performed on several lanthanide monosulfide molecules by Luo et al. [24] and spectroscopic properties of the ground state of CeS have been calculated. This calculation provided a ground state vibrational frequency of  $426 \text{ cm}^{-1}$ ; in addition, an estimate of the vibrational frequency of  $457 \text{ cm}^{-1}$  was reported based on the experimental value of CeO and some primitive calculations [25]. Contrary to the present observations, Luo et al. [24] predict a  $^3\Sigma$  ground state for CeS. The electronic structure of CeS is expected to be very similar to that of CeO for which most of the low-lying observed states were identified only by their  $\Omega$  values. The spectroscopic constants of the  $X_1$  lower state determined from the present work are:  $\omega_e = 461.3947(14)$ ,  $\omega_e x_e = 1.00095(65)$  and  $B_e'' = 0.118782207(15) \text{ cm}^{-1}$  and the constants of the  $X_2$  state are:  $\Delta G_{1/2} = 458.87411(88) \text{ cm}^{-1}$  and  $B_e'' = 0.1187649(31) \text{ cm}^{-1}$ . The equilibrium rotational constants of the two states provide equilibrium bond lengths of  $r_e'' = 2.3352875(15) \text{ \AA}$  and  $2.335399(31) \text{ \AA}$  for the two lower states. Our lower state bond lengths agree well with Luo's [24] calculated bond length of  $r_e'' = 2.36 \text{ \AA}$ .

The electronic structure and spectroscopic properties of CeS are expected to be very similar to that of CeO for which a wealth of information is available from the previous experimental and theoretical studies [9–16]. The ground  $\text{Ce}^{2+}(4f6s)0^{2-}$  configuration produces 16 electronic states, all of which have been characterized experimentally, and are supported by theoretical calculations [15]. The lowest electronic states of CeO have a pattern of  $\Omega = 2, 3, 1, 2, 0^-, 1, 0^+, 4, 3$ , and a similar pattern is expected for the lowest states of CeS. The CeS lower states observed so far have been labeled as  $X_1(3)$ ,  $X_2(\geq 2)$ ,  $X_3(\geq 2)$ ,  $X_4(\geq 3)$  and  $X_5(0)$ . At this stage we do not have any information on the relative position of the different lower states. We are also unable to decide on the ground state of CeS (although  $X_2$  or  $X_3$  are possible). It is possible that  $X_1(3)$  and  $X_2(\geq 2)$  correspond to the  $X_2(3)$  and  $X_1(2)$  states of CeO, respectively.

A review of the observed low-lying electronic states of lanthanide oxides and sulfides can provide valuable information on the electronic and configurational assignments of CeS. The low-lying states of the lanthanide oxides result from the  $4f^{N-1}6s$  configuration of the lanthanide metal ion, with the exceptions of EuO [27] and YbO [27,28]. The low-lying states of EuO and YbO arise from the  $4f^7 \text{ Eu}^+$  and  $4f^{14} \text{ Yb}^+$  configurations. Lanthanide oxides with similar ground state configurations have very similar vibrational frequencies because of the shielding properties of the  $f$  orbitals. This, therefore, provides a guide to the electron configuration. For the lanthanide oxides, all the ground state frequencies are  $\sim 820 \text{ cm}^{-1}$ , except for EuO and YbO which have ground state frequencies of  $\sim 660 \text{ cm}^{-1}$ . A similar situation is expected to hold for the sulfides. Among sulfides, HoS [7] with a ground state vibrational frequency of  $\sim 463 \text{ cm}^{-1}$  and YbS [6] with a ground state vibrational frequency of  $\sim 366 \text{ cm}^{-1}$  have been observed previously. These two have approximately the same ratio of vibrational frequencies as found for the case of the  $f^{N-1}s/f^N$  lanthanide

oxides. From this observation we conclude that the  $\sim 460 \text{ cm}^{-1}$  vibrational frequency of two of the lower states of CeS arise from the  $4f6s$  configuration of the  $\text{Ce}^{2+}$  ion. Since the first lines were not observed in any of the transitions, we would like to emphasize that the proposed electronic assignments are only tentative and further investigations are required for a more definite  $\Omega$  assignment and energy ordering of the low-lying electronic states of CeS.

#### 5. Conclusions

The emission spectra of CeS have been investigated in the  $4000\text{--}9000 \text{ cm}^{-1}$  region using a Fourier transform spectrometer. Several bands have been rotationally analyzed and classified into systems having five different lower states. Out of the observed lower states the  $X_1(3)$  and  $X_2(\geq 2)$  have very similar  $\Delta G_{1/2}$  vibrational intervals of  $459.39283(51)$  and  $458.87411(88) \text{ cm}^{-1}$ , respectively. By comparison of lower state vibrational frequencies of CeS with those of the known lanthanide oxides and sulfides, it has been concluded that the lower states arise from the ground configuration,  $\text{Ce}^{2+}(4f6s)S^{2-}$ . This work represents the first spectroscopic observation of CeS in the gas phase.

#### Acknowledgments

The research described here was supported by funds from the Leverhulme Trust of UK and the NASA laboratory astrophysics program. The spectra used in the present work were recorded at the National Solar Observatory at Kitt Peak, USA. We thank an anonymous reviewer for his very helpful comments, which greatly improved the paper.

#### Appendix A. Supplementary material

Supplementary data associated with this article can be found, in the online version, at <http://dx.doi.org/10.1016/j.jms.2014.03.003>.

#### References

- [1] R.J. Winkler Jr., S.P. Davis, M.C. Abrams, *Appl. Opt.* 35 (1996) 2874–2878.
- [2] N. Andersson, S.P. Davis, G. Edvinsson, R.J. Winkler Jr., *Phys. Scr.* 64 (2001) 134–139.
- [3] S.G. He, W.S. Tam, J.W.-H. Leung, A.S.-C. Cheung, *J. Chem. Phys.* 117 (2002) 5764–5769.
- [4] R.S. Ram, P.F. Bernath, *J. Mol. Spectrosc.* 284–285 (2013) 33–36.
- [5] T.C. Melville, J.A. Coxon, *Chem. Phys. Lett.* 318 (2000) 454–458.
- [6] T.C. Melville, J.A. Coxon, C. Linton, *J. Chem. Phys.* 113 (2000) 1771–1774.
- [7] C. Linton, A.G. Read, *J. Mol. Spectrosc.* 240 (2006) 133–138.
- [8] L.L. Ames, R.F. Barrow, *Proc. Phys. Soc.* 90 (1967) 869–870.
- [9] C. Linton, M. Dulick, R.W. Field, *J. Mol. Spectrosc.* 78 (1979) 428–436.
- [10] C. Linton, M. Dulick, *J. Mol. Spectrosc.* 89 (1981) 573–659.
- [11] C. Linton, M. Dulick, R.W. Field, P. Carette, R.F. Barrow, *J. Chem. Phys.* 74 (1981) 189–191.
- [12] C. Linton, M. Dulick, R.W. Field, P. Carette, P.C. Leyland, R.F. Barrow, *J. Mol. Spectrosc.* 102 (1983) 441–497.
- [13] L.A. Kaledin, J.E. McCord, M.C. Heaven, *J. Mol. Spectrosc.* 158 (1993) 40–61.
- [14] M. Dolg, H. Stoll, H. Preuss, *J. Mol. Struct. (Theochem)* 231 (1991) 243–255.
- [15] L.A. Kaledin, J.E. McCord, M.C. Heaven, *J. Mol. Spectrosc.* 170 (1995) 166–171.
- [16] H. Moriyama, H. Tatewaki, S. Yamamoto, *J. Chem. Phys.* 138 (2013) 224310.
- [17] R.M. Clements, R.F. Barrow, *J. Mol. Spectrosc.* 107 (1984) 119–123.
- [18] J.C. Bloch, M.C. McCarthy, R.W. Field, L.A. Kaledin, *J. Mol. Spectrosc.* 177 (1996) 251–262.
- [19] S. Wyckoff, P.A. Wehinger, *Astrophys. J.* 212 (1977) L139.
- [20] S. Wyckoff, R.E.S. Clegg, *Mon. Not. Roy. Astron. Soc.* 184 (1978) 127–143.
- [21] R.E.S. Clegg, D.L. Lambert, *Astrophys. J.* 226 (1978) 931–936.
- [22] P.S. Murthy, *Astrophys. Lett.* 23 (1983) 77–80.
- [23] P. Coppens, S. Smoes, J. Drowart, *Trans. Faraday Soc.* 63 (1967) 2140–2148.
- [24] Y. Luo, X. Wan, Y. Ito, S. Takami, M. Kubo, A. Miyamoto, *Chem. Phys.* 282 (2002) 197–206.
- [25] G. Czack, H. Hein, I. Hinz, H. Bergmann, P. Kuhn, Gmelin, *Handbook of Inorganic Chemistry*, C7, eighth ed., Springer, New York, 1983.
- [26] R.S. Ram, L. Wallace, P.F. Bernath, *J. Mol. Spectrosc.* 263 (2010) 82–88.
- [27] P. Carette, A. Hocquet, *J. Mol. Spectrosc.* 131 (1988) 301–324.
- [28] T.C. Melville, I. Gordon, K.A. Tereschuk, J.A. Coxon, P.F. Bernath, *J. Mol. Spectrosc.* 218 (2003) 235–238.